Supplemental Information

Regulation of the DNA damage response by DNA-PKcs inhibitory phosphorylation of ATM

Yi Zhou, Ji-Hoon Lee, Wenxia Jiang, Jennie L Crowe, Shan Zha, and Tanya T. Paull

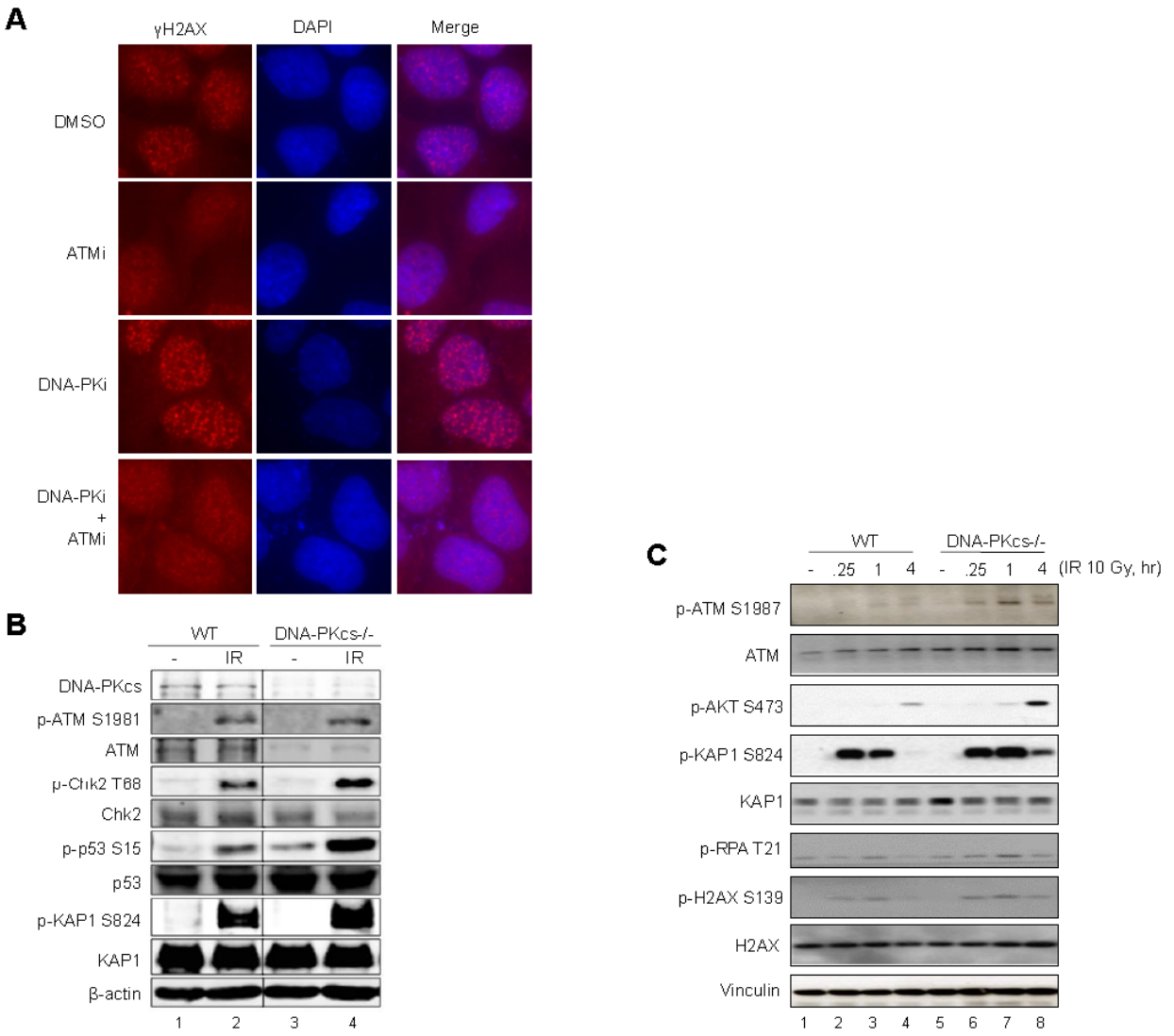

Figure S1. ATM is more active in the absence of DNA-PKcs kinase activity in mammalian cells
(A) Representative images for ER-AsiSI U2OS cells stained with DAPI, and antibody against γH2AX. The cells were pre-treated with 10 μM ATM inhibitor KU55933 (ATMi) or 10 μM DNA-PK inhibitor NU7026 (DNA-PKi) for 1 h, followed by induction of DSBs with 600 nM 4-OHT for 4 h and immunofluorescent staining.
(B) WT and DNA-PKcs-/- HCT116 cells were treated with 5 Gy ionizing radiation (IR) and incubated for 1 h, followed by western blotting analysis for the phosphorylation status of three ATM targets (phospho-Chk2(T68), phospho-p53(S15) and phospho-KAP1(S824)) .
(C) SV40 immortalized WT or DNA-PKcs-/- MEFs were untreated and irradiated (10 Gy). The cells were harvested 0.25 h, 1 h or 4 h after irradiation. Total cell lysate was analyzed by western blotting as indicated. The phosphorylation of Akt S473, which has been shown to be dependent on ATM activity (Viniegra et al., 2005), was also used as a read-out for ATM activity.

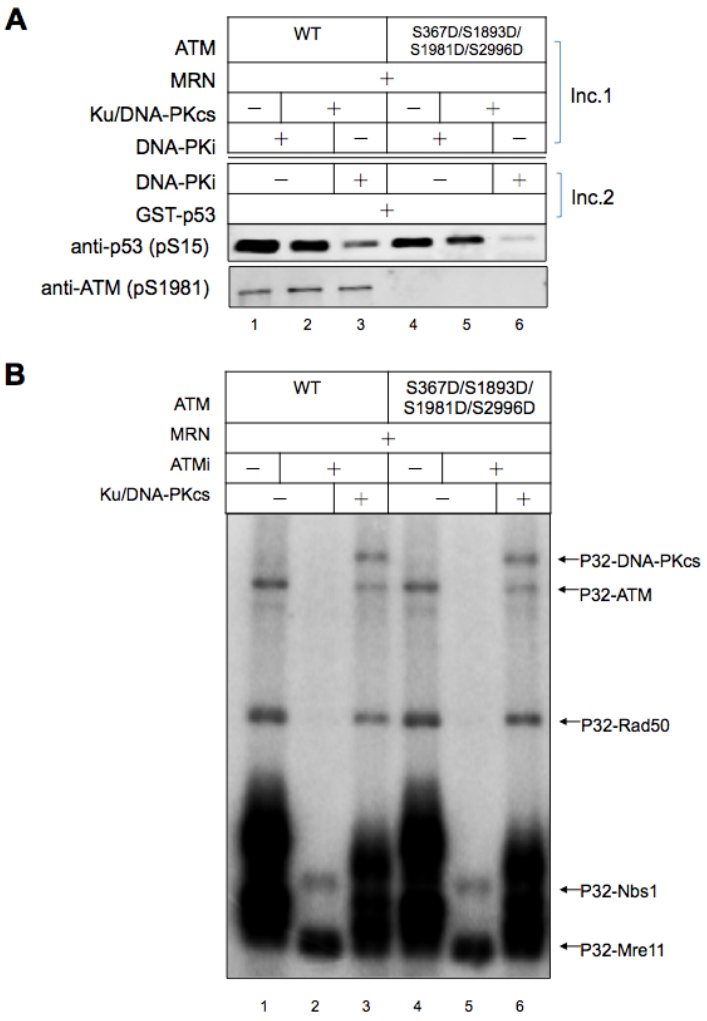

Figure S2. ATM autophosphorylation at S367/S1893/S1981/S2996 cannot overcome DNA-PKcs inhibition of ATM activity

(A) A two-step in vitro ATM kinase assay as in Figure 2B, using purified recombinant wild-type ATM (WT) or autophospho-mimetic ATM mutant S367D/S1893D/S1981D/S2996D. (B) Purified recombinant wild-type ATM (WT) or autophospho-mimetic ATM mutant S367D/S1893D/S1981D/S2996D was incubated with Ku/DNA-PKcs, MRN, linearized DNA, [γ-^{32}P]-ATP in the presence or absence of 20 μM ATM inhibitor KU55933 (ATMi). The protein products were separated on SDS-PAGE and visualized by phosphorimager.

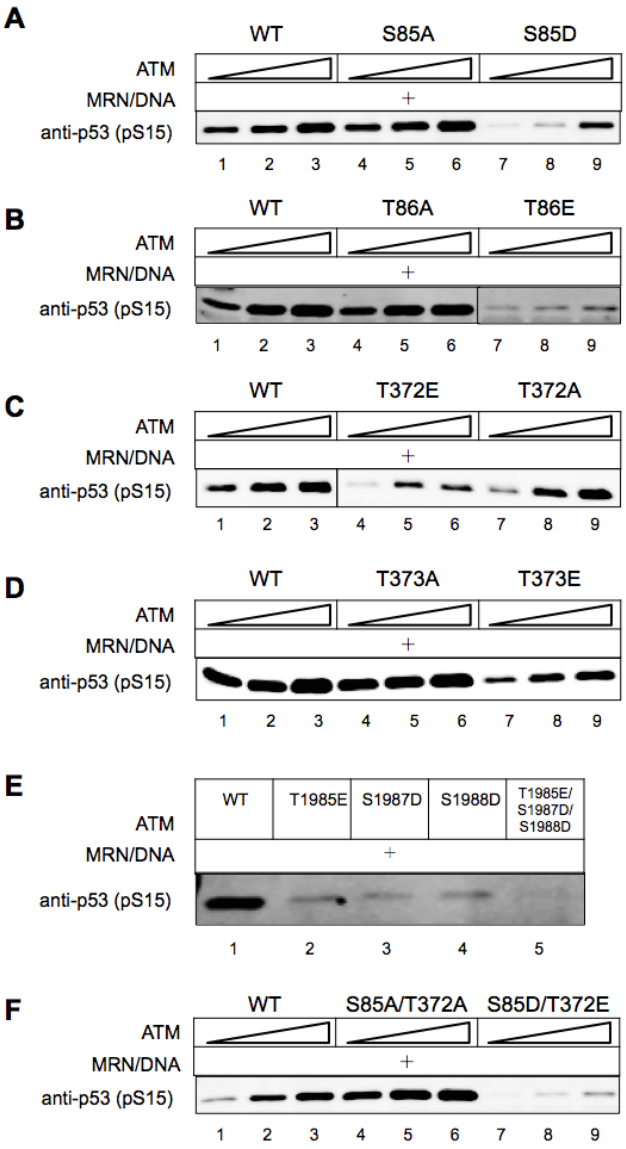

Figure S3. Characterization of ATM phosphorylation site mutants
(A) ATM phosphorylation site mutants S85A and S85D were tested in an in vitro ATM kinase assay in the presence of MRN and DNA.
(B) ATM phosphorylation site mutants T86A and T86E were tested in an in vitro ATM kinase assay in the presence of MRN and DNA.
(C) ATM phosphorylation site mutants T372A and T372E were tested in an in vitro ATM kinase assay in the presence of MRN and DNA.
(D) ATM phosphorylation site mutants T373A and T373E were tested in an in vitro ATM kinase assay in the presence of MRN and DNA.
(E) ATM phosphorylation site mutants T1985E, S1987D, S1988D and T1985E/S1987D/S1988D were tested in an in vitro ATM kinase assay in the presence of MRN and DNA.
(F) ATM phosphorylation site mutants S85A/T372A and S85D/T372E were tested in an in vitro ATM kinase assay in the presence of MRN and DNA.

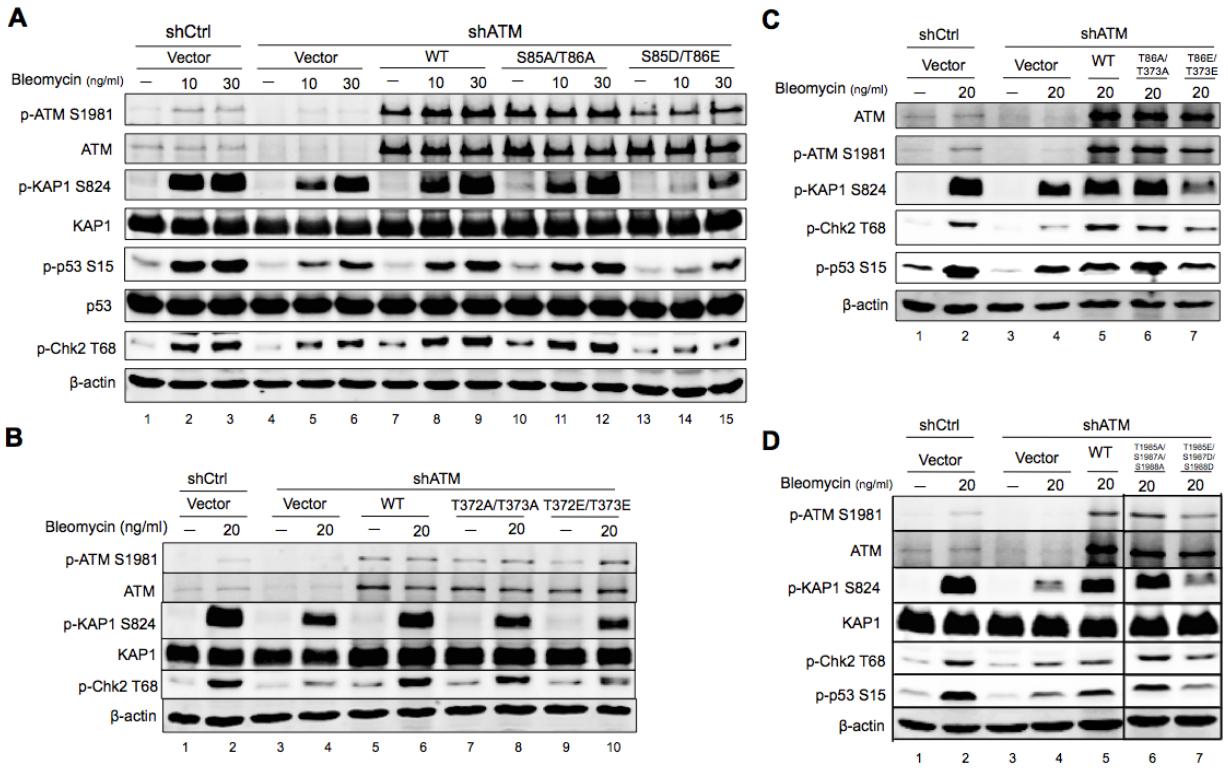

Figure S4. Examination of ATM mutants activation upon DNA damage induced by bleomycin in 293T cells
(A) Wild-type ATM (WT), phosphomimetic ATM mutant S85D/T86E, and phospho-blocking ATM mutant S85A/T86A are transiently overexpressed in 293T cells with endogenous ATM being depleted by shRNA. Cells were treated with bleomycin to induce DNA damage, followed by western blotting analysis for the phosphorylation status of three ATM targets (KAP1, p53 and Chk2). shCtrl, control shRNA; shATM, ATM shRNA.
(B) A similar experiment was performed as in (A) for Wild-type ATM (WT), phospho-mimetic ATM mutant T373E/T373E, and phospho-blocking ATM mutant T372A/T373A.
(C) A similar experiment was performed as in (A) for Wild-type ATM (WT), phospho-mimetic ATM mutant T86E/T373E, and phospho-blocking ATM mutant T86A/T373A.
(D) A similar experiment was performed as in (A) for Wild-type ATM (WT), phospho-mimetic ATM mutant T1985E/S1987D/S1988D, and phospho-blocking ATM mutant T1985A/S1987A/S1988A.

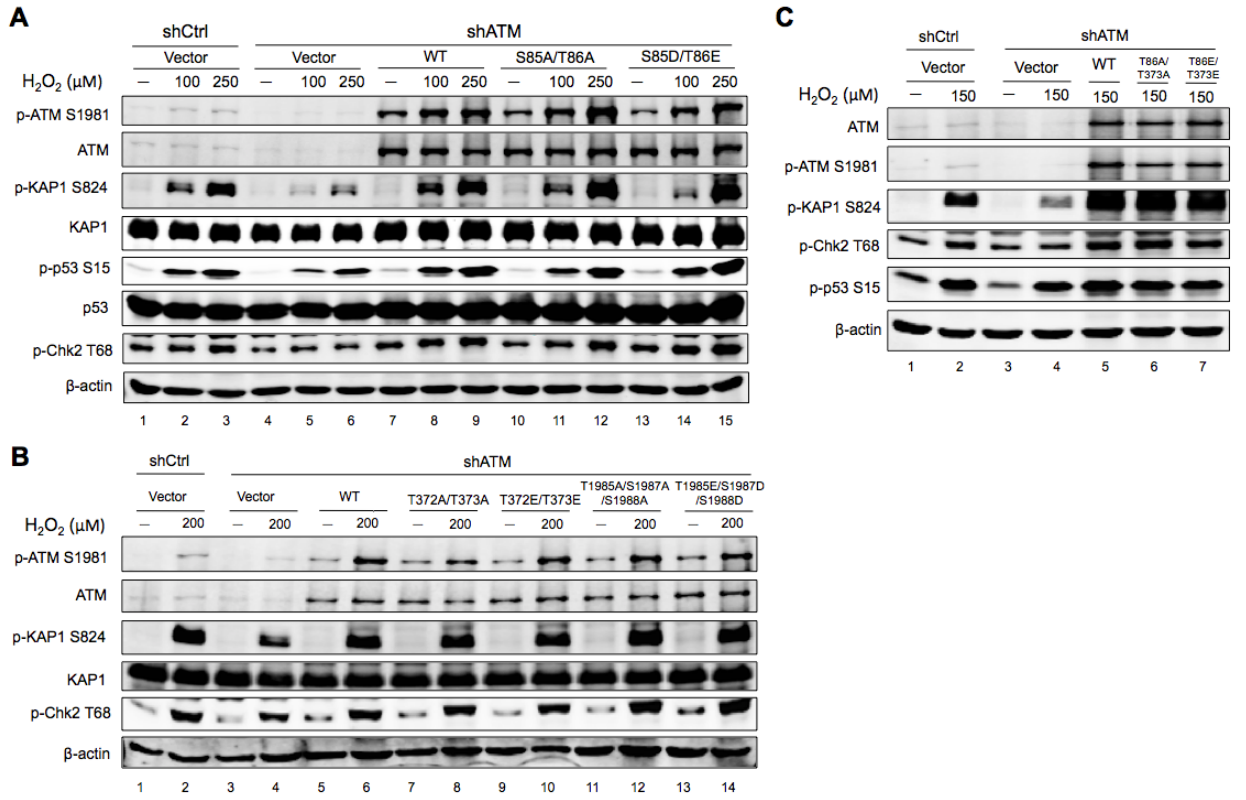

Figure S5. Examination of ATM mutants activation by H_2O_2 in 293T cells
(A) Wild-type ATM (WT), phospho-mimetic ATM mutant S85D/T86E, and phospho-blocking ATM mutant S85A/T86A are transiently overexpressed in HEK-293T cells with endogenous ATM being depleted by shRNA. Cells were treated with H_2O_2 to induce oxidative stress, followed by western blotting analysis for the phosphorylation status of three ATM targets (KAP1, p53 and Chk2). shCtrl, control shRNA; shATM, ATM shRNA.
(B) A similar experiment was performed as in (A) for Wild-type ATM (WT), phospho-mimetic ATM mutant T373E/T373E, phospho-blocking ATM mutant T372A/T373A, phospho-mimetic ATM mutant T1985E/S1987D/S1988D, and phospho-blocking ATM mutant T1985A/S1987A/S1988A
(C) A similar experiment was performed as in (A) for Wild-type ATM (WT), phospho-mimetic ATM mutant T86E/T373E, and phospho-blocking ATM mutant T86A/T373A.

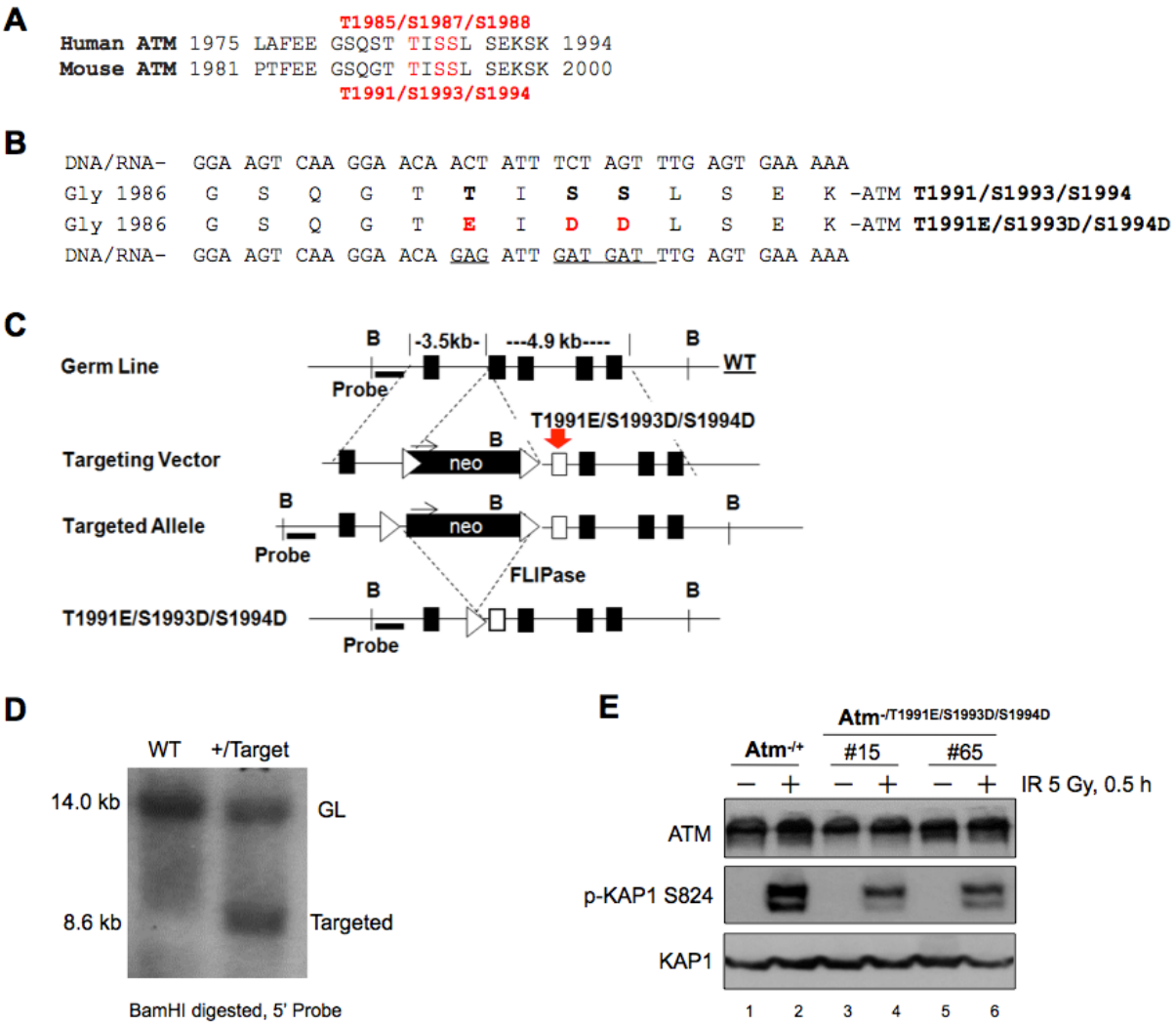

Figure S6. The effect of DNA-PKcs mediated phosphorylation on endogenous ATM activity in mouse embryonic stem (ES) cells

(A) Alignment of human and mouse ATM protein around the T1985/S1985/S1988 cluster. The corresponding amino acids for mouse ATM are T1991, S1993 and S1994 respectively.

(B) The changes on the DNA sequence to achieve the T1991E/S1993D/S1994D mutations.

(C) The targeting scheme. B = BamHI. The black boxes indicate exons. The open box marks the exon with the T1991E/S1993D/S1994D mutations. Dark line = 5' probe

(D) A representative Southern Blot showing a targeted clone (BamHI digested genomic DNA was probed by 5' probe. The germline (GL) size is 14kb and the targeting introduced a new BamHI site within the NeoR and reduced the fragment to 8.6kb.

(E) ATM+/- and two independent clones (#15 and #65) of $Atm^{-/T1991E/S1993D/S1994D}$ ES cells were irradiated at 5Gy and harvested 0.5 h later. Total ATM was blotted with anti-ATM MAT3 antibody (Sigma), p-Kap1 (S824) or total Kap1.

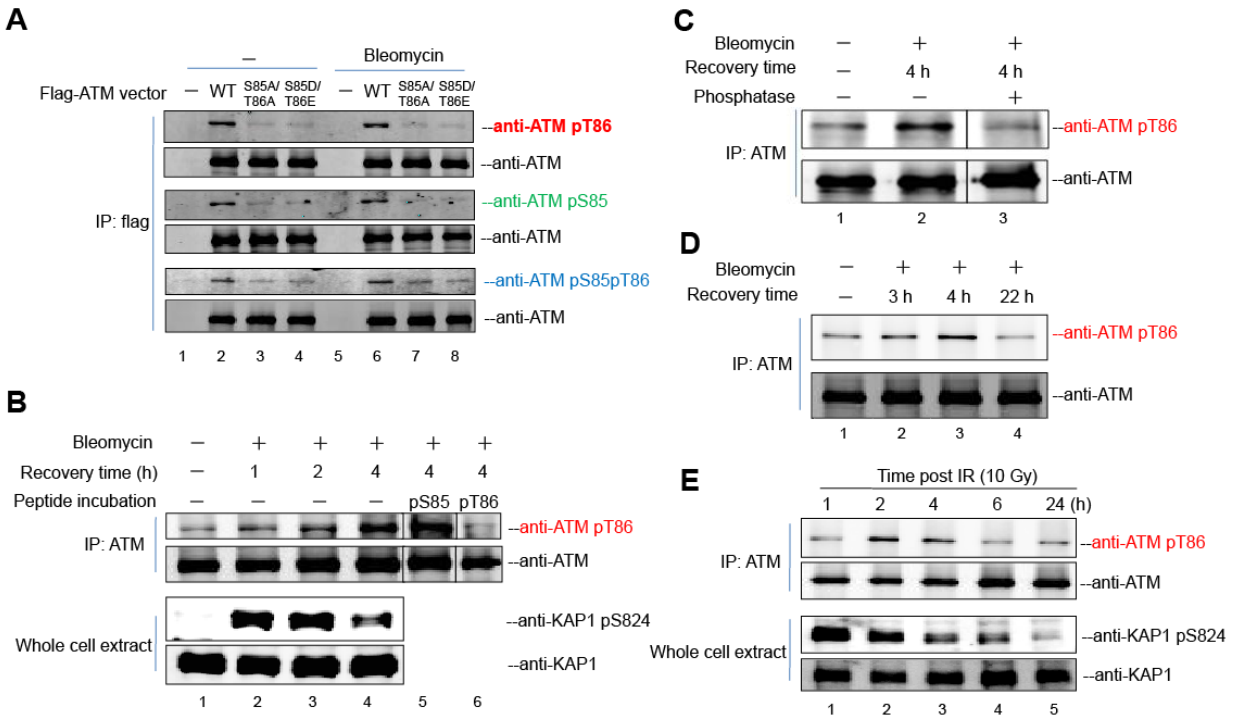

Figure S7. Phosphorylation of ATM T86 occurs in human cells

(A) Flag-tagged WT ATM and ATM mutants (S85A/T86A and S85D/T86E) were transiently overexpressed in 293T cells. Cells were treated or mocked treated with 2.5 μg/ml bleomycin for 1 h, followed by the immunoprecipitation of flag-ATM using Flag magnetic beads and detection of ATM phosphorylation using custom ATM pT86, ATM pS85 and ATM pS85pT86 antibodies.

(B) 293T cells were treated or mock treated with 2.5 μg/ml bleomycin for 1 h. After 1 h, 2 h, and 4 h of recovery, endogenous ATM was immunoprecipitated with ATM antibody and subjected to western blotting analysis using original ATM pT86 antibody or ATM pT86 antibody pre-incubated with ATM pS85 peptide or ATM pT86 peptide. The whole cell extract was blotted for KAP1 and phospho-KAP1 (S824).

(C) 293T cells were treated or mock treated with 2.5 μg/ml bleomycin for 1 h. After 4 h of recovery, endogenous ATM was immunoprecipitated with ATM antibody. One sample was treated with lambda phosphatase before western blotting.

(D) 293T cells were treated or mock treated with 2.5 μg/ml bleomycin for 1 h. After 3 h, 4 h, and 22 h of recovery, endogenous ATM was immunoprecipitated with ATM antibody and subjected to western blotting analysis.

(E) 293T cells were treated with 10 Gy IR. After 1 h, 2 h, 4 h, 6 h and 24 h of recovery, endogenous ATM was immunoprecipitated with ATM antibody and subjected to western blotting analysis. KAP1 and phospho-KAP1 (S824) were blotted in the total cell extract.

Table S1. Mass spectrometry analysis of purified ATM protein treated or mock-treated with DNA-PK

Site	Modification	Trial 1		Trial 2		References
		Total Spectra (-DNA-PK)	Total Spectra (+DNA-PK)	Total Spectra (-DNA-PK)	Total Spectra (+DNA-PK)	
S85	Phospho	-	-	-	-	Matsuoka S, et al. (2007); Kettenbach AN, et al. (2011) ; Sharma K, et al. (2014); Lee HJ, et al. (2015)
T86	Phospho	1	2	-	-	This study; Matsuoka S, et al. (2007)
S367	Phospho	2	5	-	-	This study; Matsuoka S, et al. (2007); Kozlov SV, et al. (2006)
S369	Phospho	2	1	-	-	This study
T372*	Phospho	0	1	0	2	This study
T373	Phospho	1	7	2	2	This study; Matsuoka S, et al. (2007)
S475*	Phospho	0	1	-	-	This study
T1885	Phospho	0	5	0	1	This study; Kozlov SV, et al. (2011)
S1891	Phospho	2	4	-	-	This study; Bennetzen MV, et al. (2010)
S1893	Phospho	1	0	1	0	This study; Kozlov SV, et al. (2006)
S1981		-	-	4	3	This study; Beausoleil SA, et al. (2004); Kozlov SV, et al. (2006); Matsuoka S, et al. (2007)
T1985	Phospho	0	1	-	-	This study; Matsuoka S, et al. (2007)
S1987/S1988*#	Phospho	0	1	-	-	This study
S1990*	Phospho	1	0	-	-	This study
T2396*	Phospho	1	1	-	-	This study
S2592	Phospho	5	4	-	-	This study; Lee HJ, et al. (2015)
T2978*	Phospho	3	3	-	-	This study
S2996	Phospho	2	3	-	-	This study; Daub H, et al. (2008); Kozlov SV, et al. (2011)

* Phosphorylation sites that are not reported previously
# Mass spectrometry cannot determine which site is phosphorylated

Table S2. Summary of all ATM mutants regarding kinase activity and resistance to DNA-PKcs

	ATM mutants[$]	Kinase activity (MRN/DNA)[*]	Activity repressed by DNA-PKcs?[#]
1	S367D/S1893D/S1981D/S2996D	=	Yes
2	S85A/T372A/S1885A	=	Yes
3	S85D/T372E/S1885D	↓↓↓	
4	S85A	=	Yes
5	S85D	↓↓	
6	T372A	=	Yes
7	T372E	↓	
8	S85A/T372A	=	Yes
9	S85D/T372A	↓↓↓	
10	S1885A	=	Yes
11	S1885D	=	
12	T86A	=	Yes
13	T86E	↓↓	
14	T373A	=	Yes
15	T373E	↓	
16	T86A/T373A	=	**No**
17	T86E/T373E	↓↓↓	
18	S85A/T86A	=	Yes
19	S85D/T86E	↓↓↓↓	
20	S86A/T86E	↓↓	Yes
21	S85D/T86A	↓↓	Yes
22	T372A/T373A	=	Yes
23	T372E/T373E	↓↓	
24	S474A/S475A	=	Yes
25	S475A/S2592A	=	Yes
26	S475D/S2592D	=	
27	T86A/T373A/S475A/S2592A	=	No
28	T86E/T373E/S475D/S2592D	↓↓↓	
29	S440A	=	Yes
30	S440D	=	
31	S200D	=	
32	T297E	=	
33	S1878D	=	
34	S85A/T86A/S440A	=	Yes
35	S85D/T86E/S440D	↓↓↓	
36	T1985E	↓	
37	S1987D	↓	
38	S1988D	↓	
39	T1985A/S1987A/S1988A	=	**No**
40	T1985E/S1987D/S1988D	↓↓↓	

[*] The kinase activity of each ATM mutants in the presence of MRN/DNA is tested in comparison to activity of wild-type (WT) ATM. "=" activity similar to WT; "↓" decreased activity compared with WT.

[#] The effect of DNA-PKcs on the kinase activity of ATM mutants is tested in vitro using recombinant proteins and summarized here as "Yes" for repression and "No" for no detectable inhibitory effect.

[$] Phospho-mimetic mutations at SQ/TQ sites are highlighted in red.

Supplemental Experimental Procedures

Cell Culture and Transfection

ER-*Asi*SI U2OS cells and HEK-293T cells were grown in Dulbecco's Modified Eagle Medium (Gibco) containing 10% fetal bovine serum (FBS) (Gemini). Wild-type and DNA-PKcs-/- ER-AsiSI HCT116 cells(Zhou et al., 2014) were grown in McCoy's 5A medium (Gibco) supplemented with 10% FBS and 2 mM L-glutamine (Gibco). siRNA transfection in ER-*Asi*SI U2OS cells was performed using Lipofectamine 2000 (Invitrogen) following manufacturer's instructions.HEK293-6E cells were provided by Dr. Yves Durocher and were grown in F17 medium (Gibco) supplemented with 4 mM L-Glutamine and 0.1% Pluronic F-68 (Gibco).

Establishment of ATM FLP-In U2OS Stable Cell Lines

U2OS FLP-In cells (J. Parvin) were cultured with DMEM containing 10% FBS, 100 μg/ml zeocin and 15 μg /ml blasticidin. 0.5 μg pTP3540 vector containing a wild-type ATM gene (or ATM mutant) with resistance mutations to the ATM shRNA used in this study in a plasmid derived from pcDNA5-FRT-TO (Invitrogen) was co-transfected with 4.5 μg of the pOG44 Flp-Recombinase Expression Vector into U2OS FLP-In cells. 48 h after transfection, cells were selected with 0.2 mg/ml hygromycin in DMEM containing 10% Tet System Approved FBS (Clontech, Cat No. 631106) and 15 μg /ml blasticidin for 2-3 weeks. The endogenous ATM gene was depleted by infecting the cells with ATM shRNA-expressinglentivirus overnight(GATCCGTAGCAACATACTACTCAATTCAAGAGATTGAGTAGTATGTTGCTACTTTTT-3′, sc-29761-SHC, Santa Cruz), followed by the induction of the exogenous ATM gene with 5 μg /ml doxycycline for 3-5 days. The mutant ATM constructs were generated using Quikchange mutagenesis (Thermo Fisher); details available upon request.

Protein Expression and Purification

Ku, MRN, and M(H129L/D130V)RN recombinant proteins were expressed and purified as previously described (Yang et al., 2013). Wild-type ATM and ATM mutants were expressed and purified from HEK293-6E cells (Durocher et al., 2002). Briefly, 25 μg pTT5-flag-ATM plasmid (WT or ATM mutants) was transfected into 25 ml 293-6E cells at a density of ~1.7×10^6/ml using linear polyethyleneimine (25,000 MW, Polysciences). Cells were harvested 72 h after transfection and ATM protein was purified as described previously (Peng et al., 2005). DNA-PKcs protein was a gift from Dr. Susan Lees-Miller and was purified from HeLa cells as previously described (Goodarzi and Lees-Miller, 2004).

Reagents and Antibodies

Protein kinase inhibitors used in this study were purchased from the following sources: DNA-PK inhibitor NU-7026 (Sigma, N1537), ATM inhibitor KU-55933 (EMD Millipore, 80017-420), ATR inhibitor AZ20 (Selleckchem, s7050) and DNA Ligase IV inhibitor SCR7 (Xcess Biosciences, M60082-2s). 4-Hydroxytamoxifen (4-OHT) was purchased from Sigma (Catalog no. H7904). Antibodies for western blotting and immunofluorescent staining are as follows: ATM (Santa Cruz, sc-135663), phospho-(S1981) ATM (Abcam, ab81292), p53 (Genetex,

GTX70214), phospho-(S15) p53 (Calbiochem, PC461), KAP1 (Abcam, ab22553), phospho-(S824) KAP1 (Bethyl Laboratories, A300-767A), γH2AX (Genetex, GTX80694), PARP-1 (Genetex, GTX75098), Mre11 (Genetex, GTX70212), Rad50 (Genetex, GTX70228), Nbs1 (Genetex, GTX70224), DNA-PKcs (Abcam, ab1832) and β-actin (Cell signaling, 4970).

ATM Mutagenesis

The primers for ATM mutagenesis were all designed using the online QuickChange Primer Design Program provided by Agilent Technologies; details available upon request. The mutagenesis was performed using the QuickChange XL site-directed mutagenesis kit (Agilent) using 300 ng wild-type ATM vector as a template. The QuickChange PCR products were ethanol precipitated, transformed into XL10 Gold competent cells (Agilent), and transformants were grown at 30°C.

Genomic DNA Extraction and Measurement of Resection

The extraction of genomic DNA and measurement of resection in human cells were performed as previously described (Zhou et al., 2014; Zhou and Paull, 2015). To measure the level of resection adjacent to specific DSBs, 20 μl genomic DNA sample was digested or mock digested with 20 units of restriction enzymes (BsrGI, BamHI-HF or HindIII-HF; New England Biolabs) at 37°C overnight. 3 μl digested or mock-digested samples (~20 ng) were used as templates in 25 μl qPCR reaction containing 12.5 μl 2×Taqman Universal PCR Master Mix (ABI), 0.5 μM of each primer and 0.2 μM probe using a ViiA™ 7 Real-Time PCR System (ABI). For each sample, a ‣Ct was calculated by subtracting the Ct value of the mock-digested sample from the Ct value of the digested sample. The percentage of ssDNA was calculated with the following equation: ssDNA%=1/(2^(‣Ct-1)+0.5)*100 (Zierhut and Diffley, 2008).

ATM shRNA and Control shRNA Lentivirus Packing

ATM shRNA and control shRNA lentiviruses were packed in HEK-293T cells cultured in 10-cm dishes. For each dish, 12.5 μg lentiviral vector was co-transfected with two envelope protein expressing vectors (7.5 μg pCMV-delta 8.9 and 5 μg VSV-G) into 95% confluent HEK-293T cells. After ~12 h incubation, fresh medium was added to the dish. The medium containing lentivirus was collected and filtered with 0.45 μm syringe filter after further incubation for 48 h. The lentivirus was aliquoted and stored at -80°C for future use.

RNA Interference

The DNA Ligase IV and XRCC4 siRNAs were purchased from Eurofins MWG Operon. siRNA sequences are as follows. siLigIV: AAGCCAGACAAAAGAGGUGAAdTdT (Muylaert and Elias, 2007); siXRCC4: AUAUGUUGGUGAACUGAGAdTdT (Ahnesorg et al., 2006). The transfection of siRNA was performed using Lipofectamine 2000 (Invitrogen). The efficiency of gene knockdown was examined by Western blotting 48 h after transfection.

Western Blotting

Cells were harvested and lysed in Laemmli lysis buffer (10% glycerol, 2% (m/v) SDS, 64 mM Tris-HCl pH6.8), boiled and sonicated. Protein concentrations were quantitated using BCA protein assay kit (Pierce). Proteins were separated by 6-12% SDS-PAGE, transferred to PVDF-FL membrane (Millipore), and probed with primary antibodies, followed by detection with IRDye 800 anti-mouse (Rockland, RL-610-132-121) or AlexaFluor 680 anti-rabbit (Invitrogen, A21076) secondary antibodies. Membranes were scanned using a LI-COR Odyssey scanner.

Immunofluorescence Staining

Cells were washed with PBS and fixed with 4% formaldehyde for 20 min, followed by permeabilization with cold methanol (-20 °C) for 5 min, blocking with 8% BSA for 1 h, incubation with primary antibodies (phospho-(S1981) ATM, 1:1000 dilution in 1% BSA; γH2AX, 1:750 dilution in 1% BSA) for 1 h and secondary antibodies (donkey anti-rabbit lgG Alexa Fluor 594 and donkey anti-mouse lgG Alexa Fluor 488 from Invitrogen, 1:500 dilution in 1% BSA) for 30 min at room temperature. Cells were then co-stained with DAPI (Invitrogen) and observed under a fluorescent microscope. The intensity of nuclear γH2AX foci signal and phospho-ATM S1981 foci signal were quantitated by ImageJ for each cell with at least 200 cells counted for each cell line (The fluorescent signals of each nucleus were measured in DAPI-stained area with the background being subtracted).

Protein-protein Interaction Assay

2 nM purified recombinant WT ATM or ATM mutant protein was incubated with 20 nM biotinylated MRN or MR in a 50 µl reaction in buffer A (25 mM Tris pH 8.0, 100 mM NaCl, 10% Glycerol, 1 mM DTT) for 30 min at 30 °C, followed by the addition of streptavidin dynabeads (Invitrogen) and 0.1% CHAPS. The mixture was incubated at 4 °C for 15 min with rotation. The dynabeads were washed three times with buffer A containing 0.1% CHAPS. Proteins bound to the beads were eluted by 1% SDS loading solution and analyzed by Western blotting.

Clonogenic Assay

Cells were seeded in 6-well plates at a concentration of 400 cells per well. Cells were treated with various amounts of camptothecin (CPT), H_2O_2, or ionizing radiation (IR) the next day and further cultured for 10-14 days, followed by staining the colonies with 0.5% crystal violet solution. The number of colonies in each well was quantitated and the surviving fraction was calculated by comparing the number of colonies in treated wells with the number in untreated wells.

MTT Assay

The proliferation rate of cells was determined by using the Vybrant® MTT Cell Proliferation Assay Kit (V-13154) following the manufacturer's instructions. Briefly, cells were seeded in 96-well plates at a density of 5,000 cells per well. At various time points after seeding (Day 1 to Day 5), cells were incubated with the MTT stock solution for 4 h in 37 °C incubator, followed by

dissolving the insoluble formazan product in DMSO and reading the absorbance at 540 nm using a TECAN plate reader.

Apoptosis Assay

The apoptotic rate of cells was measured with the GFP-CERTIFIED® Apoptosis/Necrosis detection kit (ENZ-51002, Enzo Life Sciences). Cells were washed with PBS twice and stained with apoptosis detection reagent (Annexin V-EnzoGold) as well as necrosis detection reagent for 30 min at room temperature. Cells were then trypsinzed and resuspended in 1X binding buffer for flow cytometric analysis.

Gene targeting in murine embryonic stem cells

To targeting the phosphomimetic mutations corresponding to T1985E/S1987D/S1988D of human ATM into murine ES cells, we aligned the mouse and human ATM protein and identified the corresponding T1991E/S1993D/S1994D sites (Figure S6A). The 5' (~3.5Kb) and 3' (~4.9 Kb) arms were PCR amplified from 129/Sv murine ES cell DNA with high fidelity DNA polymerase (Phusion, NEB). The mutations were introduced into the 3' arm with site specific mutagenesis and verified by Sanger sequencing (Figure S6B). The arms were then cloned to the pEMC targeting vector with a PGK-NeoR cassette flanked by frt sites. The targeting vector was linearized by ClaI and transfected into *ROSA26*$^{+/Cre\text{-}ERT2}$*Atm*$^{C/+}$ ES cells (Yamamoto et al., 2012). The corrected targeting brought a BamHI site within the PGK-NeoR into the Atm locus and could be identified by Southern blotting. Over 20 targeted clones were initially identified and about 60% of them have the corrected mutations based on Sanger sequencing. To distinguish whether the targeting introduced the mutation to the wildtype or the conditional allele, the targeted clones were exposed to 4OHT, which activated Cre recombination and inactivated the conditional allele. Since the PGK-NeoR cassette interferes with the transcription from the targeted ATM allele, after 4OHT treatment, the desired *Rosa26*$^{+/Cre\text{-}ERT2}$*Atm*$^{C/PGK\text{-}NeoR(T1991E/S1993D/S1994D)}$ cells would not express ATM at all, while the *Rosa26*$^{+/Cre\text{-}ERT2}$*Atm*$^{C\text{-}PGK\text{-}NeoR(T1991E/S1993D/S1994D)/+}$ cells retain ATM expression from the ATM+ allele. Two of the correctly targeted *Rosa26*$^{+/Cre\text{-}ERT2}$*Atm*$^{C/PGK\text{-}NeoR(T1991E/S1993D/S1994D)}$ ES cells were identified. Transient expression of FLipase by transfection induced recombination between the frt sites and successfully deleted the PGK-NeoR in several subclones. The resulted *Rosa26*$^{+/Cre\text{-}ERT2}$*Atm*$^{C/(T1991E/S1993D/S1994D)}$ and control parental *Rosa26*$^{+/Cre\text{-}ERT2}$*Atm*$^{C/+}$ ES cells were exposed to 4OHT for 48hrs to inactivate the AtmC and generated *Rosa26*$^{+/Cre\text{-}ERT2}$*Atm*$^{-/(T1991E/S1993D/S1994D)}$ cells used for Figure S6E.

Supplemental References

Ahnesorg, P., Smith, P., and Jackson, S.P. (2006). XLF interacts with the XRCC4-DNA ligase IV complex to promote DNA nonhomologous end-joining. Cell *124*, 301-313.

Beausoleil, S.A., Jedrychowski, M., Schwartz, D., Elias, J.E., Villen, J., Li, J., Cohn, M.A., Cantley, L.C., and Gygi, S.P. (2004). Large-scale characterization of HeLa cell nuclear phosphoproteins. Proc Natl Acad Sci U S A *101*, 12130-12135.

Bennetzen, M.V., Larsen, D.H., Bunkenborg, J., Bartek, J., Lukas, J., and Andersen, J.S. (2010). Site-specific phosphorylation dynamics of the nuclear proteome during the DNA damage response. Mol Cell Proteomics *9*, 1314-1323.

Daub, H., Olsen, J.V., Bairlein, M., Gnad, F., Oppermann, F.S., Korner, R., Greff, Z., Keri, G., Stemmann, O., and Mann, M. (2008). Kinase-selective enrichment enables quantitative phosphoproteomics of the kinome across the cell cycle. Mol Cell *31*, 438-448.

Durocher, Y., Perret, S., and Kamen, A. (2002). High-level and high-throughput recombinant protein production by transient transfection of suspension-growing human 293-EBNA1 cells. Nucleic Acids Res *30*, E9.

Goodarzi, A.A., and Lees-Miller, S.P. (2004). Biochemical characterization of the ataxia-telangiectasia mutated (ATM) protein from human cells. DNA Repair (Amst) *3*, 753-767.

Kettenbach, A.N., Schweppe, D.K., Faherty, B.K., Pechenick, D., Pletnev, A.A., and Gerber, S.A. (2011). Quantitative phosphoproteomics identifies substrates and functional modules of Aurora and Polo-like kinase activities in mitotic cells. Sci Signal *4*, rs5.

Kozlov, S.V., Graham, M.E., Jakob, B., Tobias, F., Kijas, A.W., Tanuji, M., Chen, P., Robinson, P.J., Taucher-Scholz, G., Suzuki, K.*, et al.* (2011). Autophosphorylation and ATM activation: additional sites add to the complexity. J Biol Chem *286*, 9107-9119.

Kozlov, S.V., Graham, M.E., Peng, C., Chen, P., Robinson, P.J., and Lavin, M.F. (2006). Involvement of novel autophosphorylation sites in ATM activation. EMBO J *25*, 3504-3514.

Lee, H.J., Lan, L., Peng, G., Chang, W.C., Hsu, M.C., Wang, Y.N., Cheng, C.C., Wei, L., Nakajima, S., Chang, S.S.*, et al.* (2015). Tyrosine 370 phosphorylation of ATM positively regulates DNA damage response. Cell Res *25*, 225-236.

Matsuoka, S., Ballif, B.A., Smogorzewska, A., McDonald, E.R., 3rd, Hurov, K.E., Luo, J., Bakalarski, C.E., Zhao, Z., Solimini, N., Lerenthal, Y.*, et al.* (2007). ATM and ATR substrate analysis reveals extensive protein networks responsive to DNA damage. Science *316*, 1160-1166.

Muylaert, I., and Elias, P. (2007). Knockdown of DNA ligase IV/XRCC4 by RNA interference inhibits herpes simplex virus type I DNA replication. J Biol Chem *282*, 10865-10872.

Peng, Y., Woods, R.G., Beamish, H., Ye, R., Lees-Miller, S.P., Lavin, M.F., and Bedford, J.S. (2005). Deficiency in the catalytic subunit of DNA-dependent protein kinase causes down-regulation of ATM. Cancer Res *65*, 1670-1677.

Sharma, K., D'Souza, R.C., Tyanova, S., Schaab, C., Wisniewski, J.R., Cox, J., and Mann, M. (2014). Ultradeep human phosphoproteome reveals a distinct regulatory nature of Tyr and Ser/Thr-based signaling. Cell Rep *8*, 1583-1594.

Viniegra, J.G., Martinez, N., Modirassari, P., Hernandez Losa, J., Parada Cobo, C., Sanchez-Arevalo Lobo, V.J., Aceves Luquero, C.I., Alvarez-Vallina, L., Ramon y Cajal, S., Rojas, J.M.*, et al.* (2005). Full activation of PKB/Akt in response to insulin or ionizing radiation is mediated through ATM. J Biol Chem *280*, 4029-4036.

Yamamoto, K., Wang, Y., Jiang, W., Liu, X., Dubois, R.L., Lin, C.S., Ludwig, T., Bakkenist, C.J., and Zha, S. (2012). Kinase-dead ATM protein causes genomic instability and early embryonic lethality in mice. J Cell Biol *198*, 305-313.
Yang, S.H., Zhou, R., Campbell, J., Chen, J., Ha, T., and Paull, T.T. (2013). The SOSS1 single-stranded DNA binding complex promotes DNA end resection in concert with Exo1. EMBO J *32*, 126-139.
Zhou, Y., Caron, P., Legube, G., and Paull, T.T. (2014). Quantitation of DNA double-strand break resection intermediates in human cells. Nucleic Acids Res *42*, e19.
Zhou, Y., and Paull, T.T. (2015). Direct measurement of single-stranded DNA intermediates in mammalian cells by quantitative polymerase chain reaction. Anal Biochem *479*, 48-50.
Zierhut, C., and Diffley, J.F. (2008). Break dosage, cell cycle stage and DNA replication influence DNA double strand break response. EMBO J *27*, 1875-1885.